Optica Applicata, Vol. XLVII, No. 3, 2017
DOI: 10.5277/oa170313

Optical torques and forces in birefringent microplate

C.Yu. Zenkova[1*], D.I. Ivanskyi[1], T.V. Kiyashchuk[2]

[1]Chernivtsi National University, 58012 Chernivtsi, Ukraine

[2]RUDN University, 117198 Moscow, Miklukho-Maklaya St. 6, Russia

[*]Corresponding author: k.zenkova@chnu.edu.ua

The paper presents a theoretical model for calculating the optical forces caused by the density of spin and orbital momentum and optical torque, caused by the angular momentum typical for a circularly polarized beam or a circular component of an elliptically polarized beam. Total internal reflection at the plate–air interface implemented by the birefringent plate spattered with nanoparticles of gold creates the conditions for the allocation of the predominant action of the vertical spin of the evanescent wave, which has recently been predicted theoretically.

Keywords: evanescent wave, spin angular momentum, birefringent microplate.

1. Introduction

As it is well-known, a circularly polarized beam is an example of an optical beam possessing spin angular momentum [1]. The analysis and estimation of the magnitude of such momentum are possible when it is transferred to a small particle by observing rotational or rectilinear motion of such a test object [2–12]. This feasibility is implemented for conventional, non-structured optical fields, *i.e*. plane, spherical waves *etc*. Other feasibilities are realized in the case of evanescent waves. As it has been shown in a recent paper [10], evanescent electromagnetic waves offer a rich and highly non-trivial structure of the local momentum and spin distributions. Uncommonness of the properties of evanescent waves generated by linearly polarized probing wave of azimuth 45° manifests itself, in part, in the occurrence of the vertical spin [10, 11].

In this paper, it was proposed to use the model of the computer experiment based on the birefringent plate spattered with gold nanoparticles to demonstrate and identify the vertical spin typical for an evanescent wave. Total internal reflection is realized at the border of the plate–air interface.

The results of simulation can introduce very simple and practicable technique for exploiting new, extraordinary optical phenomenon, *viz*. the presence of transverse spin momentum action of the evanescent wave arising due to total internal reflection (TIR).

2. Statement of the problem

To demonstrate the mechanical action of transversal spin currents [13, 14] inherent in the evanescent wave, we create a plane incident wave at the boundary plate–air with the azimuth of polarization ±45° with respect to the *z*-direction, as it is shown in Fig. 1.

Any movement of the plate should be performed considering the condition for realization of the vertical spin at the interface. At this case the maximal magnitude of ellipticity is achieved, while the magnitudes of the polarization components of the beam parallel and perpendicular to the plane of incidence are equal [13, 14].

The test-object is a birefringent microplate and an evanescent wave is excited just above the plate. The surfaces of a birefringent plate have negligible roughness of about 2 nm. For this reason, to transfer the transverse momentum to the plate, we deposed at its upper surface gold nanoparticles of 60 nm-diameter. The plate of size of about 200 × 200 μm is used as the test object in our model experiment.

The plate is located in the water. Total internal reflection is realized on the outside surface bordering the air. Thus at the polarization azimuth of ±45° transverse diagonal polarization-dependent force in an evanescent wave which can be transferred to the plate inducing its motion is realized.

The choice of the birefringent plate is determined by the fact the greater spectrum of optical forces due to the internal spin angular momentum, light pressure, and transverse spin of the evanescent wave can be studied for the same plate.

One can specify the following influencing factors:

i) torque arising as a result of phase difference between ordinary and extraordinary components of the probing wave that leads to changing the angular momentum and consequently the rotation of the plate;

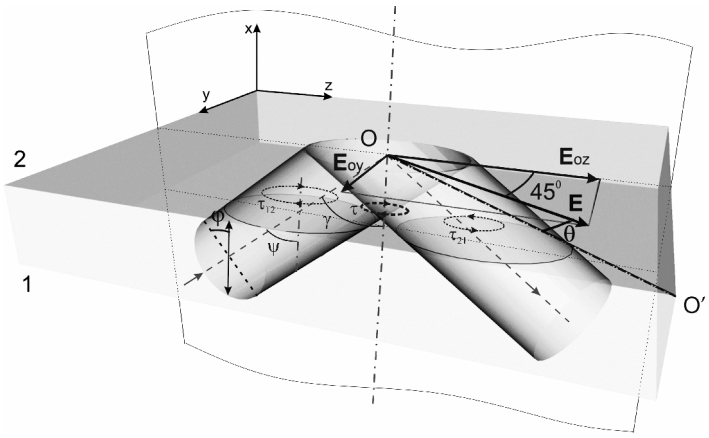

Fig. 1. Notations for the analysis of the propagation of a wave in a birefringent plane-parallel microplate; *OO′* – optical axis of a plate, γ – angle of incidence at surface 2 (plate–air interface), φ – the azimuth of polarization of the probing beam (in our case $\varphi = 45°$), θ – the angle between the optical axis of a plate and the azimuth of polarization of the wave impinging on a surface 2, ψ – angle of incidence at surface 1, τ_{12} – torque in the direction to surface 2, τ_{21} – torque in the direction to surface 1, and τ – resulting torque.

ii) torque inherent in a circularly polarized wave or circular component of an elliptically polarized wave (internal spin angular momentum);

iii) extraordinary spin angular momentum of an evanescent wave [13, 14] arising above the plate surface, being included in the complex hierarchy of the local momentum and spin distributions, here transferred to the plate that is also causing plate rotation and rectilinear motion.

Let us consider each of the above mentioned factors of influence separately.

3. Possible conditions for optical forces and torques realization

Implementation of the conditions in which the spin moment of an evanescent wave is important, presupposes the calculation of the torque related to the circular polarization due to the birefringence of the plate and subsequent compensation of these momenta. Only almost complete compensation of the momentum enables to actualize the optical power associated with the mechanical action of evanescent waves.

Let the plane *yOz* be coinciding with the plane of the plate, *cf.* Fig. 1. The linearly polarized plane probing wave is of the azimuth of polarization φ with respect to the plane of incidence. For this reason, the electric-field strength can be represented in the Cartesian coordinates as follows:

$$\mathbf{E} = \mathbf{y}E_0 \exp(-i\omega t)\sin(\varphi) + \mathbf{z}E_0 \exp(-i\omega t)\cos(\varphi)\cos(\psi)$$

where **y** and **z** are unit vectors along the axes *y* and *z*, respectively.

Here ψ is the angle of incidence to the initial surface (surface 1) of the plate. The probing beam forms a spot of area *S* at the plate. Electrical strength of the probing beam E_0 is determined by its power *P*, as:

$$\frac{P}{S} = \frac{\varepsilon_0 c}{2}E_0^2 \quad \text{or} \quad \frac{P}{S} = \frac{c}{8\pi}E_0^2$$

within the Gaussian system. Taking the angle θ between the optical axis of a crystal and the azimuth of polarization of the probing beam, one obtains [15]

$$\begin{aligned}\mathbf{E}_{\text{inc}} &= \Big\{\mathbf{y}E_0\sin(\varphi)\Big[\cos(\theta)\cos(\varphi) + \sin(\varphi)\sin(\theta)\Big] \\ &\quad + \mathbf{z}E_0\cos(\varphi)\cos(\psi)\Big[\cos(\theta)\cos(\varphi) - \cos(\theta)\sin(\varphi)\Big]\Big\}\exp(-i\omega t) \\ &= (\mathbf{y}E_y + \mathbf{z}E_z)\exp(-i\omega t)\end{aligned}$$

Beam propagation through the birefringent plate is accompanied with a phase shift between the orthogonally polarized components depending on plate thickness *d* and refraction coefficient $m' = n + i\kappa$ (for birefringence n (n_o, n_e)), where κ denotes extinction coefficient. Rotation of a plate by an angle θ with respect to the optical axis of the

crystal causes a change of orientation of the polarization ellipse with the associated change of the refraction index

$$n'_{\mathrm{e}} = \left[\frac{\sin^2(\theta)}{n_{\mathrm{e}}^2} + \frac{\cos^2(\theta)}{n_{\mathrm{o}}^2}\right]^{-1/2}$$

causing an induced path difference between the orthogonal components. Therefore, the optical path difference in the plate is likewise changed being determined by the direction of propagation of the beam in the plate γ, so that, generally, the elliptically polarized wave with the electrical vector

$$\mathbf{E}_{\mathrm{inc}_{12}} = \left\{\mathbf{y}E_y\left[\cos(\Theta)\cos(\Phi) + i\sin(\Phi)\cos(\Theta)\right]\exp\left[\frac{ikn_{\mathrm{o}}d}{\cos(\gamma)}\right]\exp\left[\frac{-k\kappa d}{\cos(\gamma)}\right]\right.$$

$$\left. + \mathbf{z}E_z\left[\sin(\Theta)\cos(\Phi) - i\cos(\Theta)\sin(\Phi)\right]\exp\left[\frac{ikn'_{\mathrm{e}}d}{\cos(\gamma)}\right]\exp\left[\frac{-k\kappa d}{\cos(\gamma)}\right]\right\}\exp(-i\omega t)$$

impinges on the second surface of the plate (surface 2 in Fig. 1). Here Φ is the degree of ellipticity of the polarization defined as the tangent of the ratio of the minor to major axes of an ellipse, Θ is the angle between the optical axis and the major axis of the ellipse of polarization, and k is the free-space wave number.

In general, the torque inherent in a plane, for elliptically polarized light wave of angular frequency ω [16] can be calculated by integration over the entire space,

$$\tau = \int(\mathbf{r} \times \langle \mathbf{T} \rangle) \cdot \hat{\mathbf{n}}\, \mathrm{d}^2 r$$

where

$$\langle \mathbf{T} \rangle = \varepsilon_0 \mathbf{E} \otimes \mathbf{E}^* + \frac{1}{\mu_0}\mathbf{B} \otimes \mathbf{B}^* - \frac{1}{2}\left(\varepsilon_0 |\mathbf{E}|^2 + \frac{1}{\mu_0}|\mathbf{B}|^2\right) I$$

is the time-averaged Maxwell stress tensor in SI-units determining the interrelation between the optical forces and the mechanical moment. Here $\otimes$ is the dyadic product, I is the unit matrix, $\hat{\mathbf{n}}$ is the surface-normal vector, $\mathbf{B} = \sqrt{\varepsilon\varepsilon_0}\,\mathbf{E}$ is the magnetic inductance vector, and ε is the media permittivity.

For computation of the torque induced in the birefringent plate we take a beam aperture 6°, determining an area of the focused beam at the plate and, correspondingly, the area of integration. A plate is divided into nanometer layers for which one computes a torque τ_{12i}.This approach facilitates taking into account the changing ellipticity for each layer. The resulting torque is found by the summation $\tau_{12} = \sum_i \tau_{12i}$, where i is the number of the layer.

The result of the simulation is shown in Fig. 2, as the dependence of the torque on the rotation angle of the plate (the rotation angle is analyzed as the deviation angle of the main axis of the plate from the initial position).

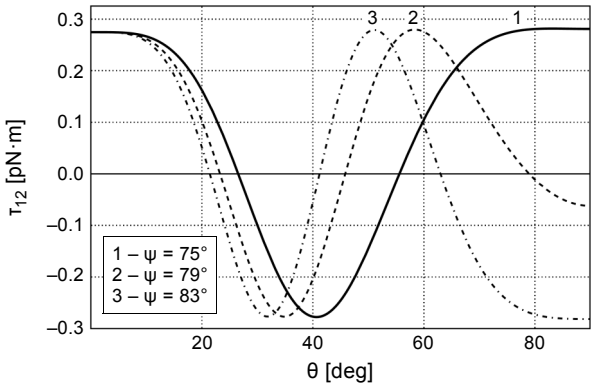

Fig. 2. The dependence of the torque of the beam in the direction to the plate–air interface on the rotation angle of the main axis of the plate for the input polarization azimuth $\varphi = 60°$ (curves correspond to different incidence angles ψ of the beam on the plate-surface 1).

Preliminary assessment of the polarization azimuth of a linearly polarized wave on the surface of the plate 1 (Fig. 2) for implementation of the vertical spin in the evanescent wave (azimuth 45° on the border of the plate–air interface) is 62°.

It should be expected that the plate rotation, at the angle of incidence on the first surface of the plate of 79°, allows realization of total internal reflection at the plate–air interface (angle 58° exceeds the critical one, which amounts to 40.5°) and the zero torque value for rotation angle of the plate is 45°. A linearly polarized wave has the zero momentum; in our case the linearly polarized wave arises when the azimuth of the polarization of the beam coincides with the main axis of the plate. On the other hand, the calculations demonstrate the formation of the azimuth of the linearly polarized wave of 45° at the plate–air interface in the case when the azimuth of the linearly polarized wave on the first surface of the plate amounts to 62°. Thus, the conditions of implementation of the decaying evanescent wave with further formation of the vertical spin in an over-surface layer of the plate were found.

Let us verify the conditions obtained for compensation of torques arising in the plate due to birefringence, taking into account the reflection of the beam from the plate–air interface. After reflection from surface 2 at the boundary plate–air, *cf*. Fig. 2, the beam propagates in the reverse direction to surface 1 governed by the condition of TIR, with the phase shift $\delta = \delta_p - \delta_s$ between the orthogonal components determined by the angle of incidence at the boundary plate–air γ. Here

$$\delta_p = -2\tan^{-1}\left[\frac{\sqrt{\sin^2(\gamma) - (n/n_o)^2}}{(n/n_o)^2\cos(\gamma)}\right]$$

$$\delta_s = -2\tan^{-1}\left[\frac{\sqrt{\sin^2(\gamma) - (n/n'_e)^2}}{\cos(\gamma)}\right]$$

As a result, a wave with the electrical vector

$$\mathbf{E}_{\mathrm{inc}_{21}} = \left\{ \mathbf{y} E_y \left[\cos(\Theta)\cos(\Phi) + i\sin(\Phi)\cos(\Theta) \right] \exp\left[\frac{i2kn_{\mathrm{o}}d}{\cos(\gamma)} \right] \exp(i\delta) \exp\left[\frac{-ik\kappa d}{\cos(\gamma)} \right] \right.$$

$$\left. + \mathbf{z} E_z \left[\sin(\Theta)\cos(\Phi) - i\cos(\Theta)\sin(\Phi) \right] \exp\left[\frac{i2kn'_{\mathrm{e}}d}{\cos(\gamma)} \right] \exp\left[\frac{-ik\kappa d}{\cos(\gamma)} \right] \right\} \exp(-i\omega t)$$

propagates in the reverse direction. By analogy with the torque τ_{12}, one computes the resulting angular momentum $\tau_{21} = \sum_i \tau_{21i}$. Changing the incidence angle leads to a change of the resulting torque $\tau = \tau_{12} + \tau_{21}$ (Fig. 3). Thus, these changes depend extensively on the rotation angle of a plate with respect to its initial orientation. For visualization of the action of the vertical spin, we intentionally look for the condition, *i.e.* the combination of magnitude of the two parameters, *viz.* the incidence angle and the angle of plate rotation, for which the optical force is largest.

Thus the action of the vertical spin becomes evident if:

i) The plate rotation stops. This occurs when under the plate rotation the azimuth of linear polarization (45°) of the incidence beam coincides with any of the plate axes;

ii) The compensation of the resulting torque τ caused by the birefringence of a plate is achieved. Figure 3 shows the results of simulation of the total angular momentum of the rotating plate at a fixed polarization azimuth at the input with the change in the angle of incidence on the first surface of the plate (curves 1, 2, and 3). Curve 2 of the figure is of particular interest as this is where one can single out a zero value of resultant momentum which occurs for the rotation angle of the plate by 45°.

Indeed, under the above mentioned conditions, the total momentum is compensated, and the plate stops and it becomes possible to distinguish the vertical spin of the evanescent wave. It is possible to select other values of rotation angles of the plate, for which there is full compensation for internal momentum induced by birefringence. But only

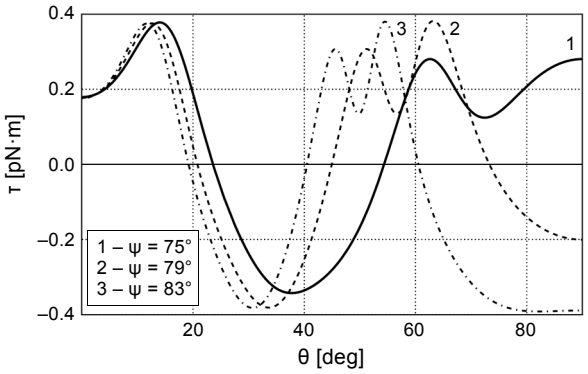

Fig. 3. Dependence of the resulting torque of the beam on the rotation angle of the main axis of the plate for polarization azimuth at the input $\varphi = 62°$ (curves correspond to different incidence angles ψ of the beam on the plate-surface 1).

for the rotation angle of 45° in this experimental model, vertical spin forming conditions are realized.

The incidence angle of 79° on the surface 1 of the plate provides the necessary conditions of visualization of the vertical spin action. It has been found that compensation of momenta is provided for incidence angles 51.5° and 58.5° when averaging over a beam aperture 6°. We choose an incidence angle of 58.5°. Subsequently, any movement of the plate can be explained by the direct action of an evanescent wave, just by mechanical action of the vertical spin arising for the azimuth of polarization ±45° of the incidence beam on the surface 2.

The next stage of the simulation is to estimate the optical power, the cause of which is the spin density of the energy flow typical for circularly polarized wave propagating through the birefringent plate. Thus we have computed the spin momentum inherent in circularly polarized wave arising in a birefringent plate for a beam propagating to the surface 2 (Fig. 1) and from this surface as a result of TIR. The results of simulation show that the magnitude of an optical force associated with a transfer of the classical spin momentum F_s inherent in circularly polarized wave and arising in the plate due to birefringence, is considerably less than a force induced by birefringence F_{br}, so that $F_s/F_{br} \approx 10^{-10}$. Thereby the intrinsic spin momentum does not affect the moving plate.

In conclusion let us estimate the value of the optical force of the evanescent wave caused by the spin and orbital momentum, at the transmission of which to over-surface gold particles the plate motion is caused.

We simulate the spin and orbital momentum density inherent in an evanescent wave when a linearly polarized incidence wave (at surface 2) with the azimuth of polarization 45° reaches the plate–air interface here undergoing TIR. The electrical vector of the impinging plane wave can be represented as

$$\mathbf{E} = E_0 \exp(-i\omega t)\left(\mathbf{x}\frac{1}{\sqrt{1+|m_1|^2}} + \mathbf{z}\frac{m}{\sqrt{1+|m_1|^2}}\right)\exp(ikz)$$

where the parameter m_1 describes the state of polarization of the probing beam being equal to unity for linear polarization with the azimuth of polarization 45°.

In this case, an evanescent wave that propagates in the z-direction, being damped in the x-direction, can be represented by [14, 17]

$$\mathbf{E}_{ev} = E\exp(-i\omega t)\left(\mathbf{x}\frac{1}{\sqrt{1+|m|^2}} + \mathbf{y}\frac{m}{\sqrt{1+|m|^2}}\frac{k}{k_z} + \mathbf{z}(-i)\frac{1}{\sqrt{1+|m|^2}}\frac{\kappa}{k_z}\right)$$

$$\times \exp(ik_z z - \kappa x)$$

where $k_z = k\dfrac{n_o}{n}\sin(\gamma)$ and the exponential decay rate $\kappa = k\sqrt{\left(\dfrac{n_o}{n}\right)^2 \sin^2(\gamma) - 1}$ (γ is the angle of incidence at the surface where TIR takes place). The state of polarization

of an evanescent wave [11] is $m = (T_\perp/T_\parallel)m_1$, where m_1 is the state of polarization of the probing beam impinging at the plate–air interface.

The electrical strength of the field of an evanescent wave is

$$E = \frac{k_z}{k}\sqrt{\frac{\mu_1}{\mu}}TE_0$$

where T is the transmission coefficient [14]

$$T = \frac{\sqrt{|T_\parallel|^2 + |m_1|^2|T_\perp|^2}}{\sqrt{1+|m_1|^2}}\exp\left[i\arg(T_\parallel)\right]$$

and $T_\parallel$ and $T_\perp$ are the Fresnel transmission coefficients.

The orbital momentum density is expressed as

$$p_\mathrm{o} \approx \mathrm{Im}\left[\mathbf{E}^*_\mathrm{ev}\cdot(\nabla)\mathbf{E}_\mathrm{ev}\right]$$

The orbital (canonical) momentum caused by light pressure determines a force transferred to the plate in the direction of propagation of an evanescent wave, here in the z-direction. Then, accordingly [18],

$$p_{oz} = A^2\left(k_z + \frac{m^2k^2}{k_z} + \frac{\kappa^2}{k_z}\right)\exp(-2\kappa x)$$

where $A = E/\sqrt{1+|m|^2}$.

An evanescent wave excited at the boundary plate–air induces the spin that is transferred to the plate causing rotation. This torque is characterized by the z- and y-directions. Then, the action of an optical force in the longitudinal z-direction is determined by the spin and orbital momentum density $F_z \approx p_{oz} + p_{sz}$, while the optical force $F_y \approx p_{sy}$ acts in the transversal y-direction.

The spin momentum is expressed as [13, 14]

$$p_\mathrm{s} = \frac{1}{2}\nabla\times\mathrm{Im}\left[\mathbf{E}^*_\mathrm{ev}\times\mathbf{E}_\mathrm{ev}\right]$$

Therefore, the longitudinal and transversal components of the spin momentum density can be written as [13]

$$p_{sy} \approx 2A^2\frac{k\kappa}{k_z}\mathrm{Im}(m)\exp(-2\kappa x)$$

$$p_{sz} \approx -2A^2\frac{\kappa^2}{k_z}\exp(-2\kappa x)$$

where $A = E/\sqrt{1+|m|^2}$.

Thus, the resulting momentum in z-direction is given by

$$p_z = p_{oz} + p_{sz} = A^2\left[k_z + \frac{m^2k^2}{k_z} + \frac{\kappa^2}{k_z} - 2\frac{\kappa^2}{k_z}\right]\exp(-2\kappa x)$$

and the transversal momentum caused by the vertical spin momentum is represented as

$$p_y = p_{sy} = 2A^2\frac{k\kappa}{k_z}\mathrm{Im}(m)\exp(-2\kappa x)$$

Changing the angle of incidence of a beam at the boundary plate–air leads to changing the ellipticity of the evanescent wave excited above the plate surface. That is why one can assume that the magnitude of the transversal spin momentum could be characterized by different dependence with respect to the resulting momentum in the longitudinal direction, where the main contribution is provided by the canonical momentum. We assume that momentum is transferred by the spherical surface S of gold particles localized at the plate surface. Light-scattering by particles is taken into account within the Mie approximation [14], giving

$$\mathbf{F} = \int_S \Delta\mathbf{p}\,\mathrm{d}S$$

where $\Delta\mathbf{p}$ is the change of momentum density. Simulation of the force affecting a plate and causing its motion presumes integration over the illuminated area assuming a beam aperture 6°.

Moreover, according to the above conditions, we select the rotation angle of the plate 45°, which corresponds to the implementation of the vertical spin.

The ratio of optical forces in the longitudinal z- and transversal y-directions for a linearly polarized incident beam with the azimuth of polarization 45° *versus* the incidence angle ψ is represented in Fig. 4 (curve 2).

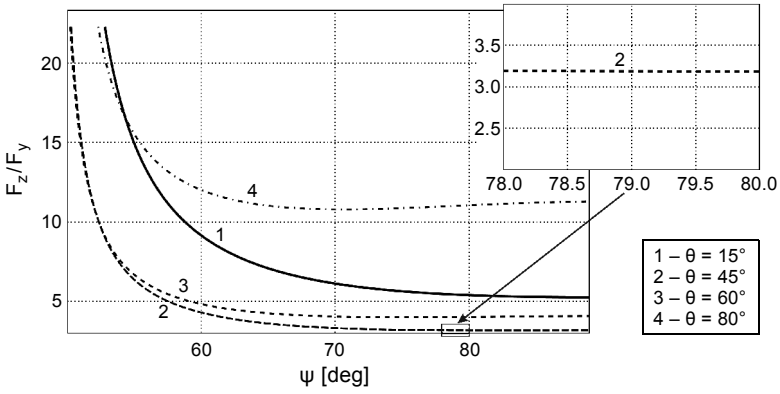

Fig. 4. The ratio of optical forces in the longitudinal and transversal directions F_z/F_y as a function of the incidence angle ψ for different azimuth of polarization of a linearly polarized wave (the increased part of curve 2 allowing to estimate the ratio of F_z/F_y at chosen modeling conditions is presented at the inset).

One can see from Fig. 4 that for some incidence angles the forces in the *y*- and *z*-directions are comparable. So, as it can be seen from this figure (curve 2, the insert), for the incidence angle of about 79° one obtains $F_z/F_y \approx 3.2$. This is just the angle, for which the momentum caused by birefringence (for the beams propagating to the boundary plate–air and from this boundary) is compensated. That is why one can regard the motion of a plate in a direction different from longitudinal as the result of the action of an optical force, one of the components of which is the force induced by the transversal spin momentum.

Thus, the result of the above theoretical modeling consists in determining the conditions that can be used in a real experiment for demonstrating unusual mechanical action of evanescent waves.

4. Conclusions

The main result of this research is the realization of computer prediction of the existence of conditions under which the mechanical action of the vertical spin of the evanescent wave becomes obvious at irradiation of the "birefringent plate–air" interface by a linearly polarized wave of the azimuth 45°. Selecting the birefringent plate, as the model sample, enabled to analyze the full set of forces that arise and are caused by birefringence due to the intrinsic properties of a circularly polarized wave, and by manifestations of the action of the spin and orbital energy flows of the evanescent wave.

The compensation condition (incidence angle of 79°) of the torque occurring due to birefringence in the plate when the subsequent motion of the plate is caused only by the action of the vertical spin of the evanescent wave was found. It was observed that at a certain selected incidence angle the ratio of the longitudinal component of the optical force in the evanescent wave, the components of which are the longitudinal components of the orbital and the spin momenta, is three times greater than the value of the transverse component of the spin momentum. As a result, the motion of the plate due to the action of the transverse spin momentum becomes obvious.

References

[1] OHANIAN H.C., *What is spin?*, American Journal of Physics **54**(6), 1986, pp. 500–505.

[2] BERRY M.V., *Optical currents*, Journal of Optics A: Pure and Applied Optics **11**(9), 2009, article ID 094001.

[3] ANGELSKY O.V., BEKSHAEV A.YA., MAKSIMYAK P.P., MAKSIMYAK A.P., MOKHUN I.I., HANSON S.G., ZENKOVA C.YU., TYURIN A.V., *Circular motion of particles suspended in a Gaussian beam with circular polarization validates the spin part of the internal energy flow*, Optics Express **20**(10), 2012, pp. 11351–11356.

[4] ANGELSKY O.V., BEKSHAEV A.YA., MAKSIMYAK P.P., MAKSIMYAK A.P., HANSON S.G., ZENKOVA C.YU., *Orbital rotation without orbital angular momentum: mechanical action of the spin part of the internal energy flow in light beams*, Optics Express **20**(4), 2012, pp. 3563–3571.

[5] BARNETT S.M., BERRY M.V., *Superweak momentum transfer near optical vortices*, Journal of Optics **15**(12), 2013, article ID 125701.

[6] ANGELSKY O.V., BEKSHAEV A.YA., MAKSIMYAK P.P., MAKSIMYAK A.P., HANSON S.G., ZENKOVA C.YU., *Self-action of continuous laser radiation and Pearcey diffraction in a water suspension with light -absorbing particles*, Optics Express **22**(3), 2014, pp. 2267–2277.

[7] POLYANSKII V.K., ANGELSKY O.V., POLYANSKII P.V., *Scattering-induced spectral changes as a singular optical effect*, Optica Applicata **32**(4), 2002, pp. 843–848.

[8] ANGELSKY O.V., BEKSHAEV A.YA., MAKSIMYAK P.P., MAKSIMYAK A.P., HANSON S.G., ZENKOVA C.YU., *Self-diffraction of continuous laser radiation in a disperse medium with absorbing particles*, Optics Express **21**(7), 2013, pp. 8922–8938.

[9] ANGELSKY O.V., USHENKO A.G., USHENKO YE.G., TOMKA YU.Y., *Polarization singularities of biological tissues images*, Journal of Biomedical Optics **11**(5), 2006, article ID 054030.

[10] ANGELSKY O.V., TOMKA YU.Y., USHENKO A.G., USHENKO YE.G., YERMOLENKO S.B., USHENKO YU.A., *2-D tomography of biotissue images in pre-clinic diagnostics of their pre-cancer states*, Proceedings of SPIE **5972**, 2005, article ID 59720N.

[11] ANGELSKY O.V., BESAHA R.N., MOKHUN A.I., MOKHUN I.I., SOPIN M.O., SOSKIN M.S., VASNETSOV M.V., *Singularities in vectoral fields*, Proceedings of SPIE **3904**, 1999, pp. 40–54.

[12] ANGELSKY O.V., GORSKY M.P., HANSON S.G., LUKIN V.P., MOKHUN I.I., POLYANSKII P.V., RYABIY P.A., *Optical correlation algorithm for reconstructing phase skeleton of complex optical fields for solving the phase problem*, Optics Express **22**(5), 2014, pp. 6186–6193.

[13] ANTOGNOZZI M., BERMINGHAM C.R., HARNIMAN R.L., SIMPSON S., SENIOR J., HAYWARD R., HOERBER H., DENNIS M.R., BEKSHAEV A.Y., BLIOKH K.Y., NORI F., *Direct measurements of the extraordinary optical momentum and transverse spin-dependent force using a nano-cantilever*, Nature Physics **12**(8), 2016, pp. 731–735.

[14] BLIOKH K.Y., BEKSHAEV A.Y., NORI F., *Extraordinary momentum and spin in evanescent waves*, Nature Communications **5**, 2014, article ID 3300.

[15] FRIESE M.E.J., NIEMINEN T.A., HECKENBERG N.R., RUBINSZTEIN-DUNLOP H., *Optical alignment and spinning of laser-trapped microscopic particles*, Nature **394**(6691), 1998, pp. 348–350.

[16] ROCKSTUHL C., HERZIG H.P., *Calculation of the torque on dielectric elliptical cylinders*, Journal of the Optical Society of America A **22**(1), 2005, pp. 109–116.

[17] HAYAT A., MUELLER J.P.B., CAPASSO F., *Lateral chirality-sorting optical forces*, PNAS Early Edition **112**(43), 2015, pp. 13190–13194.

[18] BEKSHAEV A.YA., ANGELSKY O.V., SVIRIDOVA S.V., ZENKOVA C.YU., *Mechanical action of inhomogeneously polarized optical fields and detection of the internal energy flows*, Advances in Optical Technologies, Vol. 2011, 2011, article ID 723901.

Received January 30, 2017
in revised form February 22, 2017